Modeling of Cascaded Coplanar Waveguide Discontinuities by the Mode-Matching Approach

Rolf Schmidt and Peter Russer, *Fellow, IEEE*

Abstract— **Cascaded coplanar waveguide discontinuities with transverse dimensions in the order of some micrometers are analyzed by the mode-matching and generalized scattering matrix method. This approach permits a full-wave analysis of the electromagnetic field also in the metallic regions. Compared with full-wave analysis assuming perfect conductors and a subsequent loss computation based on the surface impedance model the accuracy is considerably enhanced.**

The mode-matching method is revisited in the context of a network representation of discontinuities. The implications of Tellegen's general network theorem on the mode-matching method, particularly on the testing functions, are investigated. Furthermore, the mode-matching method is related to the equivalence principle applied to discontinuites and to the continuity condtion of voltage and current of quasi-TEM waves in the static approximation.

I. Introduction

IN MONOLITHIC MICROWAVE integrated circuit design coplanar waveguide (CPW) structures meet with growing interest. In recent publications the influence of the metallization thickness on the scattering characteristics of cascaded CPW discontinuities is investigated [1], [6]. The results confirm that the finite metallization thickness may significantly affect the electrical characteristics of CPW circuits. However, these approaches are based on field modelling assuming perfect conductors, which is only valid for waveguides with transverse dimensions considerably larger than the skin depth. In CPW's with strip width and metallization thickness in the skin depth's order of magnitude conductor loss influences the propagation characteristics of transmission lines [2]–[5] and hence the scattering behavior of cascaded discontinuities. A full-wave analysis is required considering also the electromagnetic field inside the conductor. The present analysis is based on the generalized scattering matrix method and the mode-matching method. This approach permits a fully self-consistent description of the conductor losses. The eigenmodes of the waveguides as well as the scattering behavior of cascaded discontinuities are computed by this method.

Modes are matched at boundaries by applying the method of moments [8] to the continuity condition of the tangential field components. Truncating the complete set of eigenmodes numerical results depend on the set of testing functions used in the method of moments. Usually the modal magnetic field vector functions of one side of the discontinuity are employed for testing the continuity of the tangential electric field and the electric field vector functions of the other side are used for enforcing the continuity of the tangential magnetic field [1], [5], [10]. According to the experimentally verified boundary enlargement/reduction concept in [10] one of these two sets can be specified, which gives the fastest convergence of the solution. This set is rigorously justified in [11] by an investigation of the matching equations with regard to their linear independence.

In this paper the mode-matching method is revisited by considering Tellegen's general network theorem [12] to the equivalent network representation of the discontinuity. Using the above stated testing functions it is proven that Tellegen's theorem applies to the generalized voltages and currents of the modes irrespective of the number of modes retained in the mode-matching approach. The coupling of the eigenmodes can thus be modelled by a multiport which contains only a connection network including ideal transformers. This property implies the symmetry and orthogonality of the generalized scattering matrix and in lossless waveguides also the conservation of complex power across the discontinuity. The difficulty in choosing the appropiate set of testing functions out of the two nominated is rigorously resolved by relating the mode-matching method to the reaction concept [13] applied to equivalent current densities in the discontinuity plane. From the assumption of a not vanishing electric equivalent current on the conductors the set of testing functions can be specified, which permits this condition of the equivalent electric current. These testing functions correspond to those stated by [11]. A further justification of these testing functions is yielded from the condition that enforcing the continuity condition of the tangential field components by the single mode-matching approach must lead to the continuity of the well-defined voltage and current in the static approximation.

II. Method of Analysis

We consider the cascaded waveguide discontinuity in Fig. 1, which is enclosed inside a rectangular box with perfect electric conducting walls. The cascaded waveguide discontinuity consists of three waveguide sections. The location of the discontinuity plane between two waveguides i and j is denoted by z_{ij}. The electromagnetic fields in the waveguide i can be

Manuscript received March 1, 1995; revised July 10, 1995. This work was supported by the Siemens AG, Munich.

The authors are with the Technische Universität München, Lehrstuhl für Hochfrequenztechnik, Arcisstraße 21, 80290 München, Germany.

IEEE Log Number 9415462.

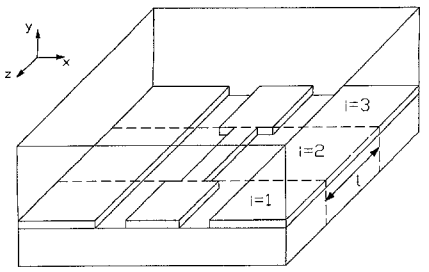

Fig. 1. Cascaded coplanar waveguide discontinuities enclosed in rectangular box with perfect conducting walls.

expanded in terms of the respective eigenmodes. Suppose $\boldsymbol{e}_{tn}^{(i)}$ and $\boldsymbol{h}_{tn}^{(i)}$ are the normalized transverse electric and magnetic modal field vector functions, respectively. Taking N^i eigenmodes into account the transverse fields in the waveguide i may be expressed by

$$\boldsymbol{E}_t^{(i)} = \sum_{n=1}^{N^i} \sqrt{Z_{Wn}^{(i)}}\left(a_n^{(i)}(z) + b_n^{(i)}(z)\right)\boldsymbol{e}_{tn}^{(i)}(x,y), \quad (1)$$

$$\boldsymbol{H}_t^{(i)} = \sum_{n=1}^{N^i} \sqrt{Y_{Wn}^{(i)}}\left(a_n^{(i)}(z) - b_n^{(i)}(z)\right)\boldsymbol{h}_{tn}^{(i)}(x,y) \quad (2)$$

where $a_n^{(i)}$ and $b_n^{(i)}$ are the wave amplitudes of the nth eigenmode in waveguide i and $Z_{Wn}^{(i)} = (Y_{Wn}^{(i)})^{-1}$ are real positive normalization constants. The following orthogonality relation holds for the normalized modal field vector function over the waveguide cross-section S^i

$$\iint_{S^i} \boldsymbol{e}_{tm}^{(i)} \times \boldsymbol{h}_{tn}^{(i)} \cdot \boldsymbol{n}_z \, dS = \delta_{mn} \quad (3)$$

$\boldsymbol{n}_z$ is the unit vector in z-direction. Introducing generalized voltages $V_n^{(i)}$ and currents $I_n^{(i)}$ the field expansion (1), (2) can be written as

$$\boldsymbol{E}_t^{(i)}(x,y,z) = \sum_{n=1}^{N_i} V_n^{(i)}(z)\boldsymbol{e}_{tn}^{(i)}(x,y), \quad (4)$$

$$\boldsymbol{H}_t^{(i)}(x,y,z) = \sum_{n=1}^{N_i} I_n^{(i)}(z)\boldsymbol{h}_{tn}^{(i)}(x,y). \quad (5)$$

A. Generalized Network Representation

We introduce an equivalent circuit representation of the discontinuity where the discontinuity itself is described by a connection multiport. In this multiport, which may contain ideal transformers, energy is neither stored nor dissipated. Each port k represents an eigenmode of the waveguides i and j, respectively. The number of ports of the connection circuit is equal to $N = N^i + N^j$, which is the number of considered eigenmodes on both sides of the discontinuity. At any time t Tellegen's theorem [12] is fulfilled by the port voltages $v_k(t)$ and currents $i_k(t)$ of the connection circuit

$$\sum_{k=1}^{N} v_k(t)i'_k(t) = 0, \quad \sum_{k=1}^{N} v'_k(t)i_k(t) = 0. \quad (6)$$

The voltages $v'_k(t)$ and currents $i'_k(t)$ may also represent excitations of the circuit different from the excitation given by $v_k(t)$ and $i_k(t)$. If we define the vectors

$$\boldsymbol{V} = \begin{bmatrix} \boldsymbol{V}^{(i)} \\ \boldsymbol{V}^{(j)} \end{bmatrix} \quad \text{and} \quad \boldsymbol{I} = \begin{bmatrix} \boldsymbol{I}^{(i)} \\ \boldsymbol{I}^{(j)} \end{bmatrix} \quad (7)$$

where $\boldsymbol{V}^{(i)}$ and $\boldsymbol{I}^{(i)}$ are column vectors with the complex elements $V_n^{(i)}(z_{ij})$ and $I_n^{(i)}(z_{ij})$, we obtain the following two relations for the complex voltages and currents of the external ports of the network

$$\boldsymbol{V}^T \cdot \boldsymbol{I}' = 0, \quad (8)$$

$$\boldsymbol{V}^T \cdot (\boldsymbol{I}')^* = 0. \quad (9)$$

$\boldsymbol{V}$ and $\boldsymbol{I}'$ are vectors in the complex N-dimensional vector space $\mathbb{C}^N$. The set of all potential voltage and current vectors at the external ports span the subspaces $\mathbb{K}_V^{N_1}$ and $\mathbb{K}_I^{N_2}$. The dimensions N_1 and N_2 of these two subspaces depend on the internal structure of the connection network. Since (9) holds $\mathbb{K}_V^{N_1}$ and $\mathbb{K}_I^{N_2}$ are orthogonal subspaces of $\mathbb{C}^N$. From (8) it follows that the voltage subset $\mathbb{K}_V^{N_1}$ and the set of conjugate current vectors $\boldsymbol{I}^*$, denoted by $\mathbb{K}_{I^*}^{N_2}$, constitute also orthogonal subspaces of $\mathbb{C}^N$.

B. Generalized Scattering Matrix

The coupling between the eigenmodes in the discontinuity plane can be characterized by a generalized scattering matrix $\boldsymbol{S}$:

$$\boldsymbol{b} = \boldsymbol{S}\boldsymbol{a}. \quad (10)$$

Properties of the generalized scattering matrix (GSM) of the equivalent multiport can be established from the two statements (8) and (9) of Tellegen's theorem. From (8), which implies the conservation of the self-reaction $\iint_S \boldsymbol{E}_t \times \boldsymbol{H}_t \cdot \boldsymbol{n}_z \, dA$ across the discontinuity, the following two properties can be found

$$\boldsymbol{S} = \boldsymbol{S}^T, \qquad \boldsymbol{S}^T\boldsymbol{S} = \mathbf{1} \quad (11)$$

where $\mathbf{1}$ is the unit matrix. The GSM of a multiport representing a waveguide discontinuity is symmetric and orthogonal. From (9) the unitary of the scattering matrix $\boldsymbol{S}$ can be proven

$$\boldsymbol{S}\boldsymbol{S}^\dagger = \mathbf{1} \quad (12)$$

where "$\dagger$" denotes the hermitian conjugate matrix.

C. Mode-Matching at Waveguide Discontinuities

The elements of the GSM can be determined by enforcing the continuity of the tangential field components across the

step discontinuity. This condition can be written as

$$\sum_{n=1}^{N^i} V_n^{(i)} \boldsymbol{n}_z \times \boldsymbol{e}_n^{(i)} = \sum_{n=1}^{N^j} V_n^{(j)} \boldsymbol{n}_z \times \boldsymbol{e}_n^{(j)}, \tag{13}$$

$$\sum_{n=1}^{N^i} I_n^{(i)} \boldsymbol{n}_z \times \boldsymbol{h}_n^{(i)} = -\sum_{n=1}^{N^j} I_n^{(j)} \boldsymbol{n}_z \times \boldsymbol{h}_n^{(j)}. \tag{14}$$

In order to solve (13), (14) by the method of moments [14], an inner product between two vector functions $\boldsymbol{u}(x, y)$ and $\boldsymbol{v}(x, y)$ is introduced and defined as

$$\langle \boldsymbol{u}, \boldsymbol{v} \rangle = \iint_S \boldsymbol{u}^\dagger \boldsymbol{v} \, dS. \tag{15}$$

Testing the continuity of the tangential electric and magnetic field components by N_e vector functions $\boldsymbol{w}_m^E$ and N_h vector functions $\boldsymbol{w}_m^H$, respectively, the two following matrix equations arise

$$\boldsymbol{W}_E^{(i)} \boldsymbol{V}^{(i)} = \boldsymbol{W}_E^{(j)} \boldsymbol{V}^{(j)}, \tag{16}$$

$$\boldsymbol{W}_H^{(i)} \boldsymbol{I}^{(i)} = -\boldsymbol{W}_H^{(j)} \boldsymbol{I}^{(j)} \tag{17}$$

with the matrices $[\boldsymbol{W}_E^{(i)}]_{mn} = \langle \boldsymbol{w}_m^E, \boldsymbol{n}_z \times \boldsymbol{e}_n^{(i)} \rangle$ and $[\boldsymbol{W}_H^{(i)}]_{mn} = \langle \boldsymbol{w}_m^H, \boldsymbol{n}_z \times \boldsymbol{h}_n^{(i)} \rangle$. Since we need N independent equations to describe uniquely a N-port [18], the total number of required testing functions is

$$N_e + N_h = N. \tag{18}$$

Substituting the generalized voltages and currents by wave amplitudes the GSM can be easily derived from the above matrix equations. In order to condense these equations, we define the matrices $\boldsymbol{W}_E = [\boldsymbol{W}_E^{(i)}, -\boldsymbol{W}_E^{(j)}]$ and $\boldsymbol{W}_H = [\boldsymbol{W}_H^{(i)}, \boldsymbol{W}_H^{(j)}]$. Hence we get

$$\boldsymbol{W}_E \boldsymbol{V} = \boldsymbol{0}, \tag{19}$$

$$\boldsymbol{W}_H^* \boldsymbol{I}^* = \boldsymbol{0}. \tag{20}$$

The set of vectors $\boldsymbol{V}$ satisfying the N_e equations of (19) constitute the $N_1 = N - N_e$-dimensional subspace $\mathbb{K}_V^{N_1}$ of the complex vector space $\mathbb{C}^N$ and the set of solution vectors $\boldsymbol{I}^*$ of the N_h equations (20) constitute a $N_2 = N - N_h$-dimensional subspace $\mathbb{K}_{I^*}^{N_2}$. Due to (18) the sum of the dimensions of these two vector spaces is N. Representing the coupling of the eigenmodes by an equivalent multiport Tellegen's theorem must apply to these subspaces. Due to (8) subspaces $\mathbb{K}_V^{N_1}$ and $\mathbb{K}_{I^*}^{N_2}$ must be orthogonal. Since the sum of their dimensions is N both subspaces are complementary with respect to $\mathbb{C}^N$. By utilizing finite dimensional linear algebra it can be shown that the subspace spanned by the complex conjugate row vectors of the matrix $\boldsymbol{W}_E$ is also complementary to $\mathbb{K}_V^{N_1}$ [17]. Hence, any current vector $\boldsymbol{I}^*$ may be expressed as a linear combination of the row vectors of the matrix $\boldsymbol{W}_E^*$ in the form $\boldsymbol{I}^* = \boldsymbol{W}_E^\dagger \alpha$. In the same way the relation $\boldsymbol{V} = \boldsymbol{W}_H^T \beta$ must be valid. Inserting these two linear combinations into (19) and (20) we obtain $\boldsymbol{W}_E \boldsymbol{W}_H^T \beta = 0$ and $\boldsymbol{W}_H^* \boldsymbol{W}_E^\dagger \alpha = 0$. Since these equations must hold for any α and any β, it follows

$$\boldsymbol{W}_E \boldsymbol{W}_H^T = \boldsymbol{0}. \tag{21}$$

Taking the orthogonality relation (3) into account it can be easily shown that the condition (21) can be fulfilled by the two sets (A) and (B) of testing functions

$$\text{(A):} \quad \begin{aligned} \boldsymbol{w}_m^E &= \boldsymbol{h}_m^{(i)*}, \quad N_e = N^i, \\ \boldsymbol{w}_m^H &= \boldsymbol{e}_m^{(j)*}, \quad N_h = N^j, \end{aligned} \tag{22}$$

$$\text{(B):} \quad \begin{aligned} \boldsymbol{w}_m^E &= \boldsymbol{h}_m^{(j)*}, \quad N_e = N^j, \\ \boldsymbol{w}_m^H &= \boldsymbol{e}_m^{(i)*}, \quad N_h = N^i. \end{aligned} \tag{23}$$

Using testing functions from either set (A) or (B) the complex statement (8) of Tellegen's theorem will be satisfied for both sets. For discontinuities between waveguides with different apertures, however, only one set is appropiate according to [11], since the other set yields linearly dependent equations. Specifically, for waveguide discontinuities which are characterized by the aperture relation $S_a^j \subset S_a^i$ the choice of testing functions used in the field matching must be set (A). The aperture S_a^i is hereby defined as the set of points of the waveguide cross-section S_i, which are not located in the conductor regions. The aperture relation between the waveguides 1 and 2 in Fig. 1 can thus be denoted by $S_a^1 \subset S_a^2$. In the following we shall give a further justification of this criterion. The equivalence principle allows the separation of the discontinuity problem into a pair of equivalent problems [16]. In each problem, the equivalent electric and magnetic current densities, $\boldsymbol{J}$ and $\boldsymbol{M}$, must be equal to the discontinuities in the tangential field, from the actual field in one waveguide to zero in the other. The original problem is the superposition of these two equivalent configurations. The current densities are not yet known. They are determined by expanding them into a series of appropiate functions. The expansion coefficients can be found from the condition that the surface currents produce null fields in one waveguide in each problem. It can be shown easily that using $\boldsymbol{n}_z \times \boldsymbol{h}_n^{(i)}$ as the expansion functions for $\boldsymbol{J}$ and $\boldsymbol{e}_n^{(j)} \times \boldsymbol{n}_z$ for $\boldsymbol{M}$ the follwing current densities are obtained

$$\text{(A):} \quad \boldsymbol{J} = \sum_{n=1}^{N^i} I_n^{(i)} \boldsymbol{n}_z \times \boldsymbol{h}_n^{(i)}, \quad \boldsymbol{M} = \sum_{n=1}^{N^j} V_n^{(j)} \boldsymbol{e}_n^{(j)} \times \boldsymbol{n}_z. \tag{24}$$

Using the Lorentz reciprocity theorem the generalized voltages $V_n^{(i)}$ can be deduced from $\boldsymbol{M}$ and the currents $I_n^{(j)}$ from $\boldsymbol{J}$

$$V_n^{(i)} = -\langle \boldsymbol{h}_n^{(i)}, \boldsymbol{M} \rangle, \tag{25}$$

$$I_n^{(j)} = \langle \boldsymbol{e}_n^{(j)}, \boldsymbol{J} \rangle. \tag{26}$$

These equations are identical with the (16) and (17), if the testing functions of set (A) are applied in the mode-matching method. Because of this analogy the expansion (24) is also denoted by (A). In the same way the current expansion

$$\text{(B):} \quad \boldsymbol{J} = \sum_{n=1}^{N^j} I_n^{(j)} \boldsymbol{n}_z \times \boldsymbol{h}_n^{(j)}, \quad \boldsymbol{M} = \sum_{n=1}^{N^i} V_n^{(i)} \boldsymbol{e}_n^{(i)} \times \boldsymbol{n}_z \tag{27}$$

leads to (16) and (17), if testing functions from set (B) are employed. This correspondence between the sets of testing functions and the equivalent current densities in the discontinuity plane yields a rigorous justification for the above stated choice of testing functions. Specifically, matching fields between waveguides $i = 1$ and $j = 2$ in Fig. 1 we have to use the testing functions of set (B), because only the equivalent electric current density $\boldsymbol{J}$ is not vanishing on the conductors. This selection of testing functions can also be justificated by the requirement that imposing the continuity condition of the tangential field components of quasi-TEM waves by the mode-matching method must lead to the continuity of the well-defined voltage and current in the static approximation.

D. Matching of Quasi-TEM Waves

In the static approximation the transverse modal electric and magnetic fields can be expressed by the gradients of skalar potentials $\Phi^{(i)}$ and $\Psi^{(i)}$, respectively. Taking only the quasi-TEM waves into account, the continuity condition of the tangential fields (13) tested with the functions from set (A) can be written as

$$V_1^{(i)} \iint_{S_a^i} \nabla_t \Phi^{(i)} \cdot \nabla_t \Psi^{(i)} \times \boldsymbol{n}_z \, dS = V_1^{(j)} \iint_{S_a^i} \nabla_t \Phi^{(j)} \cdot \nabla_t \Psi^{(i)} \times \boldsymbol{n}_z \, dS. \quad (28)$$

Making use of the vector identity $\nabla_t \Phi \cdot (\nabla_t \Psi \times \boldsymbol{n}_z) = \nabla_t \cdot [\Phi(\nabla_t \Psi \times \boldsymbol{n}_z)]$ and the two-dimensional divergence theorem, both surface integrals can be converted into contour integrals along the surface of the inner and outer conductor. Since the electric potential is constant on these boundaries $\Phi^{(i)}$ and $\Phi^{(j)}$ may be extracted from both integrals, respectively. Provided the magnetic potential $\Psi^{(i)}$ is defined on the inner and outer conductor contours of both waveguides, which is the case for $S_a^j \subset S_a^i$, the contour integral of the magnetic fields can be canceled in the continuity condition of the tangential electric fields. Expressing the electric potential difference by a line integeral, (28) can be rewritten as

$$V_1^{(i)} \int_{C_e^i} \boldsymbol{e}_{tn}^{(i)} \cdot d\boldsymbol{l} = V_1^{(j)} \int_{C_e^j} \boldsymbol{e}_{tn}^{(j)} \cdot d\boldsymbol{l}. \quad (29)$$

This equation implies the continuity of the voltage. In the same way the continuity condition of the magnetic fields (14), tested by the same set (A) of functions, can be transformed into the following equation, which expresses the continuity of the current

$$I_1^{(i)} \int_{C_h^i} \boldsymbol{h}_{tn}^{(i)} \cdot d\boldsymbol{l} = -I_1^{(j)} \int_{C_h^j} \boldsymbol{h}_{tn}^{(j)} \cdot d\boldsymbol{l}. \quad (30)$$

Note that the derivations of (29) and (30) for discontinuities with $S_a^j \subset S_a^i$ only hold, if the testing functions of set (A) are used in the mode-matching method. Correspondingly, for discontinuities with $S_a^i \subset S_a^j$ the testing functions of set (B) must be taken in order to yield the continuity of the voltage and current in the static approximation.

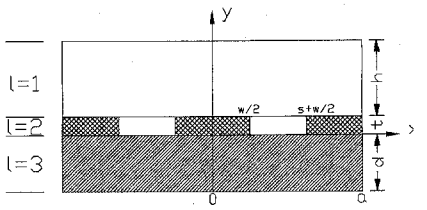

Fig. 2. Coplanar waveguide cross section.

E. Calculation of the Eigenmodes

In Fig. 2 a coplanar waveguide (CPW) with finite metallization thickness inside a rectangular box with perfect electric conducting walls is depicted. Due to the symmetry with respect to the plane $x = 0$, only half of the structure has to be considered. The cross section is divided into three layers. In each of the layers l the modal field vector functions $\boldsymbol{e}_n^{(i,l)}$ and $\boldsymbol{h}_n^{(i,l)}$ of the n-th eigenmode may be expanded into a sum of LSE_x and LSH_x partial wave components. These waves can be determined in closed-form expressions [4]. Taking $\overline{N}_i^l$ partial waves of layer l into account, we get

$$\boldsymbol{n}_y \times \boldsymbol{e}_n^{(i,l)}(x,y) = \sum_{\nu=1}^{\overline{N}_i^l} \overline{V}_{n\nu}^{(i,l)}(y) \boldsymbol{n}_y \times \overline{\boldsymbol{e}}_{n\nu}^{(i,l)}(x), \quad (31)$$

$$\boldsymbol{n}_y \times \boldsymbol{h}_n^{(i,l)}(x,y) = \sum_{\nu=1}^{\overline{N}_i^l} \overline{I}_{n\nu}^{(i,l)}(y) \boldsymbol{n}_y \times \overline{\boldsymbol{h}}_{n\nu}^{(i,l)}(x) \quad (32)$$

where $\overline{\boldsymbol{e}}_{n\nu}^{(i,l)}$ and $\overline{\boldsymbol{h}}_{n\nu}^{(l)}$ are the vector-valued expansion functions for the electric and magnetic field respectively. The field expansions in two neighboring layers l and k are matched by applying the method of moments to the tangential field continuity conditions

$$\boldsymbol{n}_y \times (\boldsymbol{e}_n^{(i,l)} - \boldsymbol{e}_n^{(i,k)}) = 0, \quad \boldsymbol{n}_y \times (\boldsymbol{h}_n^{(i,l)} - \boldsymbol{h}_n^{(i,k)}) = 0 \quad (33)$$

at their horizontal boundary. Hence we define another inner product

$$\langle \boldsymbol{u}, \boldsymbol{v} \rangle = \int_0^a \boldsymbol{u}^\dagger \boldsymbol{v} \, dx. \quad (34)$$

Defining $\overline{\boldsymbol{e}}_{-n\nu}^{(i,l)}$ and $\overline{\boldsymbol{h}}_{-n\nu}^{(i,l)}$ as the expansion functions of the electromagnetic field which propagates in the opposite z-direction the following orthogonality relations hold

$$\langle (\overline{\boldsymbol{e}}_{-n\mu}^{(i,l)})^*, \boldsymbol{n}_y \times \overline{\boldsymbol{h}}_{n\nu}^{(i,l)} \rangle = \delta_{\mu\nu}, \quad (35)$$

$$\langle (\overline{\boldsymbol{e}}_{-n\mu}^{(i,l)})^*, \boldsymbol{n}_y \times \overline{\boldsymbol{h}}_{n\nu}^{(i,l)} \rangle = \delta_{\mu\nu}. \quad (36)$$

Hence the coupling of the partial waves of neighboring layers can be analyzed by the same formalism applied to waveguide discontinuities. Specifically, a generalized scattering matrix associated to an equivalent multiport can be introduced, which characterizes the coupling of the partial waves. If we truncate the field expansions in the layers to a finite number of partial waves it can be shown in the same way as in section C that Tellegen's theorem apply to the generalized voltages $\overline{\boldsymbol{V}}_{n\nu}^{(i,l)}$ and currents $\overline{\boldsymbol{I}}_{n\nu}^{(i,l)}$. In this case the tangential electric field is tested by a number of $\overline{N}_e$ functions $\overline{\boldsymbol{w}}_\mu^E$ and the magnetic

field by a number of $\overline{N}_h$ functions $\overline{\boldsymbol{w}}_\mu^H$. This set (A) of testing functions is given by

$$(\overline{\mathrm{A}}):\quad \overline{\boldsymbol{w}}_\mu^E = (\overline{\boldsymbol{h}}_{-n\mu}^{(i,l)})^*,\quad \overline{N}_e = \overline{N}_i^l,$$
$$\overline{\boldsymbol{w}}_\mu^H = (\overline{\boldsymbol{e}}_{-n\mu}^{(i,k)})^*,\quad \overline{N}_h = \overline{N}_i^k. \tag{37}$$

Again there exists also another set (B) of testing functions, given by

$$(\overline{\mathrm{B}}):\quad \overline{\boldsymbol{w}}_\mu^E = (\overline{\boldsymbol{h}}_{-n\mu}^{(i,k)})^*,\quad \overline{N}_e = \overline{N}_i^k,$$
$$\overline{\boldsymbol{w}}_\mu^H = (\overline{\boldsymbol{e}}_{-n\mu}^{(i,l)})^*,\quad \overline{N}_h = \overline{N}_i^l. \tag{38}$$

In the same way as for the waveguide discontinuity corresponding equivalent current densities $\overline{\boldsymbol{J}}_n$ and $\overline{\boldsymbol{M}}_n$ can be introduced to describe the continuity conditions between the layers l and k of the waveguide i

$$(\overline{\mathrm{A}}):\quad \overline{\boldsymbol{J}}_n = \sum_{\nu=1}^{\overline{N}_i^l} \overline{I}_{n\nu}^{(i,l)} \boldsymbol{n}_y \times \overline{\boldsymbol{h}}_{n\nu}^{(i,l)},$$
$$\overline{\boldsymbol{M}}_n = \sum_{\nu=1}^{\overline{N}_i^k} \overline{V}_{n\nu}^{(i,k)} \overline{\boldsymbol{e}}_{n\nu}^{(i,k)} \times \boldsymbol{n}_y, \tag{39}$$

$$(\overline{\mathrm{B}}):\quad \overline{\boldsymbol{J}}_n = \sum_{\nu=1}^{\overline{N}_i^k} \overline{I}_{n\nu}^{(i,k)} \boldsymbol{n}_y \times \overline{\boldsymbol{h}}_{n\nu}^{(i,k)},$$
$$\overline{\boldsymbol{M}}_n = \sum_{\nu=1}^{\overline{N}_i^k} \overline{V}_{n\nu}^{(i,l)} \overline{\boldsymbol{e}}_{n\nu}^{(i,l)} \times \boldsymbol{n}_y. \tag{40}$$

Due to this analogy testing functions of set $(\overline{\mathrm{A}})$ must be chosen in the field matching procedures between the layers $l = 1$ and $k = 2$, because the not vanishing electric current on the surface of metallization layer can be modelled only by this set. Accordingly the field matching between the layers $l = 2$ and $k = 3$ is performed using the testing functions of set $(\overline{\mathrm{B}})$. By combining all continuity equations and boundary conditions at the horizontal waveguide walls at $y = -d$ and $y = t + h$ a sufficient number of equations is obtained to determine the complex propagation constants k_z and the unknown partial wave amplitudes of the fundamental and higher-order modes.

III. Numerical Results

A computer program has been developped to deal with cascaded discontinuities of waveguides, which may be modelled by an arbitrary composition of layers enclosed in a rectangular box with perfect conducting walls. First we calculated the propagation characteristics of a CPW with a metallization thickness which is not large in comparison with the skin depth. The CPW was measured by R. B. Marks from the NIST. The experimental data are taken from [7]. In Figs. 3 and 4 the frequency dependence of the propagation and attenuation constant is plotted and compared with the results of a full-wave field analysis assuming perfect conductors. In this case conductor loss is computed by modelling the field inside the conductor by a surface impedance and a surface impedance matrix description. In the surface impedance matrix

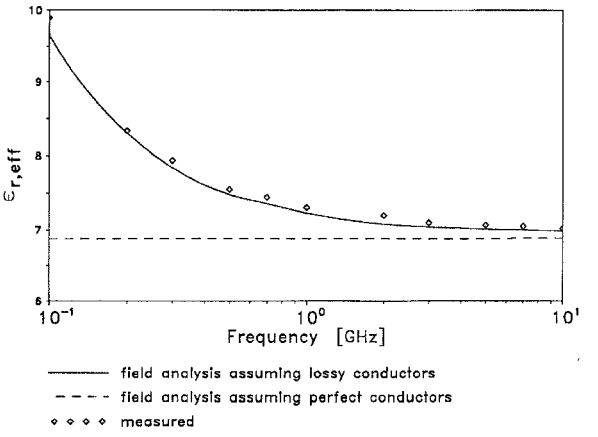

Fig. 3. Effective dielectric constant of CPW (metallization: $w = 71$ μm, $s = 49$ μm; $t = 1.61$ μm, $\sigma = 3 \cdot 10^7$ S/m; subtrate: $d = 500$ μm, $\epsilon_r = 12.9$, $\tan\ \delta = 3 \cdot 10^{-4}$).

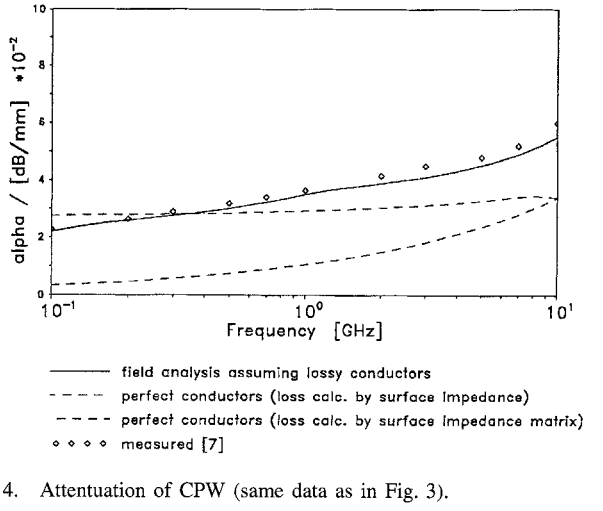

Fig. 4. Attentuation of CPW (same data as in Fig. 3).

description the coupling of the fields on top and bottom of the metallization layer is taken into account. In Fig. 3 the relative effective permittivity $\epsilon_{r,\mathrm{eff}}$ exhibits a negative slope over the whole frequency band. This behavior can only be modelled by field analysis taking into account also the metallic losses.

The scattering characteristics of cascaded waveguide discontinuities are calculated by combining successively the GSM's of the waveguide step discontinuities and of the waveguide transmissions lines between the junctions [15]. By using this approach higher-order mode interactions between junctions are included. We calculated the reflection coefficient of cascaded CPW step discontinuities using the same parameters as Alessandri *et al.* [6], who considered the metallization layer a perfect conductor and verified their results by experiments. The results of both calculations are shown in Fig. 5. As can be seen, the results agree excellently, thus confirming the validity of the mode-matching approach described above.

Fig. 6 shows the dependence of the fundamental mode scattering parameters of cascaded CPW discontinuites on the distance L between the discontinuities for perfect and

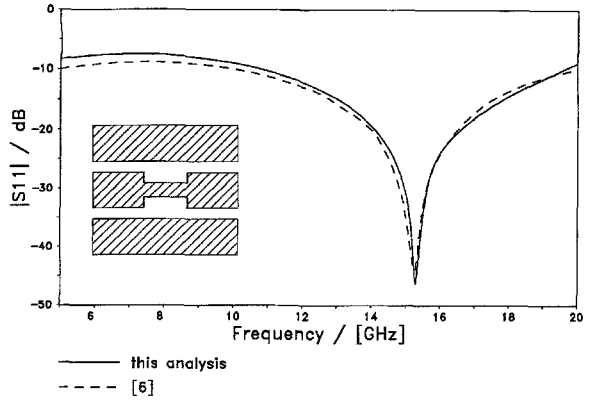

Fig. 5. Comparison of computed return loss of double step discontinuity in CPW. (Feeding line: $w_1 = w_3 = 0.5$ mm, $s_1 = s_3 = 0.2$ mm. Central line: $w_2 = 0.2$ mm, $w_2 = 0.35$ mm. Distance between steps: $L = 4.36$ mm. Substrate: $d = 0.635$ mm, $\epsilon_r = 9.9$. Metallization thickness $t = 35$ μm. Housing: WR28.)

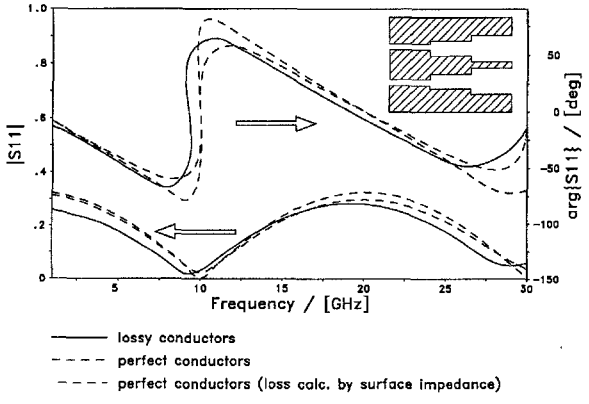

Fig. 6. S_{11} of cascaded CPW discontinuity (metallization: $w1 = w3 = 15$ μm,$w2 = 20$ μm, $s1 = s2 = 10$ μm,$s2 = 5$ μm,$t1 = t2 = t3 = 0.2$ μm,$\sigma = 2 \cdot 10^7$ S/m; substrate: $d = 200$ μm,$\epsilon_r = 12.9$,tan $\delta = 1 \cdot 10^{-4}$; frequency: $f = 10$ GHz).

non-perfect conductors. The attenuation of the fundamental eigenmode of the inner waveguide b with a perfect metallization layer is hereby approximated by the two surface impedance models. The periodic variation of the scattering parameter S_{11} in Fig. 6 indicates the existence of a standing wave between the two cascaded discontinuities [1]. Fig. 6 shows that the resonant behavior in a CPW with transverse dimensions, which are not large compared to the skin depth, can be correctly modelled only by a self-consistent description of the metallic losses.

Figs. 7 and 8 show the scattering characteristics of a 35–70 Ω quarter-wave transformer over the frequency for perfect and non-perfect conductors. Fig. 7 also shows the results, if we assume perfect conductors in the field analysis and compute the attentuation of the waveguides by the surface impedance approximation. The various results differ significantly. The deviation is due to the following two effects: Metallic loss influences the propagation constant of the quarter-wave matching waveguide and thus the frequency of the reflection minimum. As Fig. 9 shows, metallic loss affects also the scattering characteristics of the waveguide transitions and hence of the composite structure.

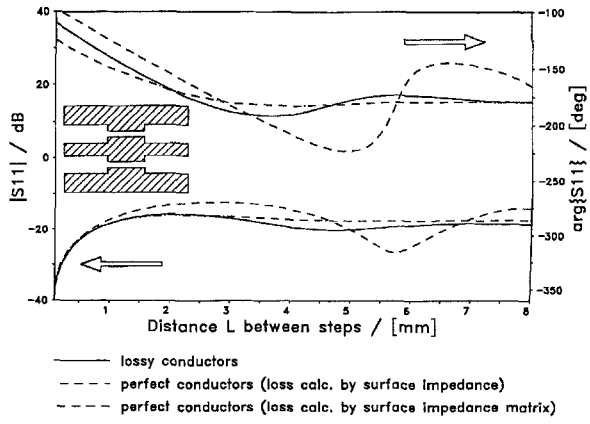

Fig. 7. Reflection coefficient of $\lambda/4$ transformer (substrate: $\epsilon_r = 12.9$, thickness: 200 μm. metallization thickness: 3 μm. waveguide 35 Ω : $w = 20$ μm, $s = 5$ μm. waveguide 50 Ω: $w = 15$ μm, $s = 10$ μm, $l = 3.104$ mm. waveguide 70 Ω: $w = 8$ μm, $s = 17$ μm.)

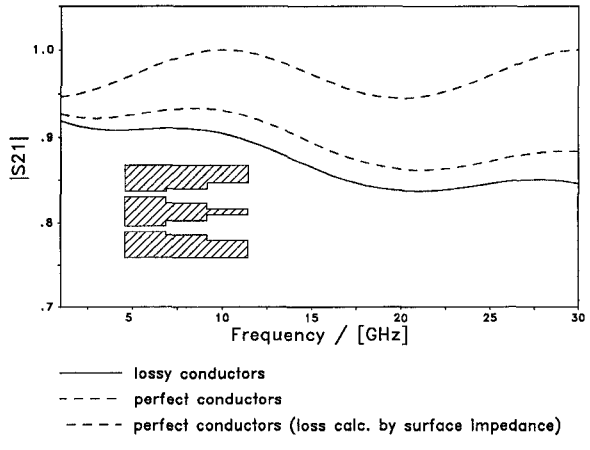

Fig. 8. Transmission coefficient of $\lambda/4$ transformer (same data as in Fig. 7).

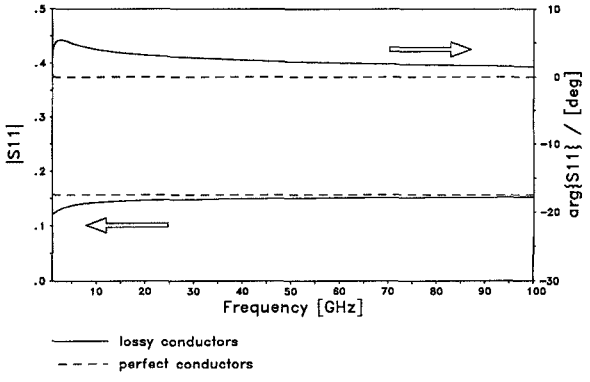

Fig. 9. Scattering parameters of 35–50 Ω waveguide transition (data from Fig. 7).

In Fig. 10 the transmission coefficient of a low-pass filter of 11th order is plotted over the frequency band. In such a composite structure the above stated deviations accumulate leading to the strong difference in the scattering characteristics of the filter.

The computer programm is also able to handle multilayer waveguides, which allow very compact passive filter structures [9]. Fig. 12 shows such a structure, which constitutes a low-

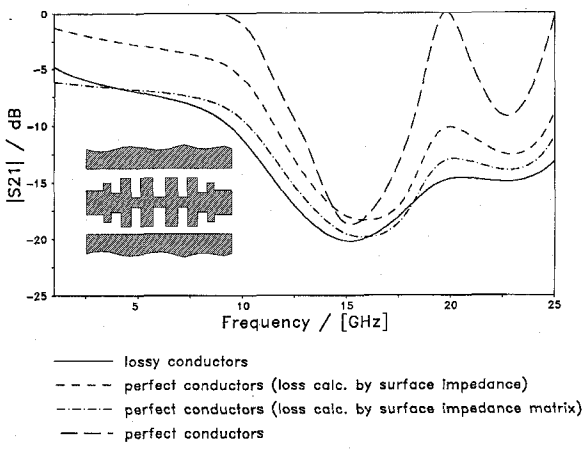

Fig. 10. $\cdot\,|S21|$ of low-pass filter of 11th order (subtrate: $\epsilon_r = 12.9$, thickness $= 500\ \mu\text{m}, \tan\ \delta = 1 \cdot 10^{-4}$. metallization thickness $t = 1.0\ \mu\text{m}$, distance between ground metallization layers $w + 2s = 42\ \mu\text{m}, \sigma = 2 \cdot 10^7$ S/m).

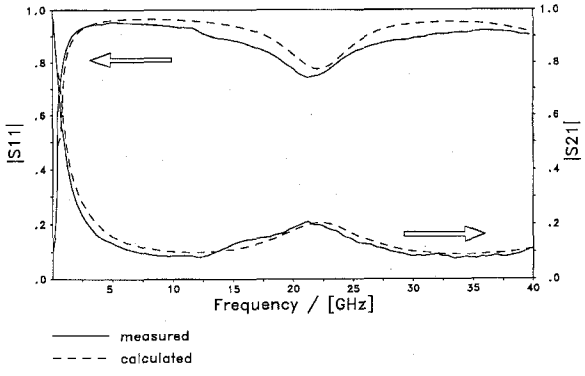

Fig. 11. Scattering parameters of multilayer waveguide structure ($w = 100\ \mu\text{m}, s = 128\ \mu\text{m}$, metallization thickness: $1\ \mu\text{m}, \sigma = 1.7 \cdot 10^7$ S/m, $l = 3.25$ mm, $d1 = 2.5\ \mu\text{m}, d2 = 400\ \mu\text{m}, \epsilon_r = 12.95$).

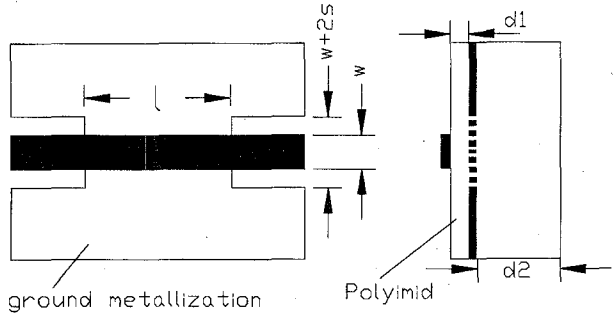

Fig. 12. Multilayer waveguide structure.

impedance microstip line between two coplanar waveguides. The reflection and transmission coefficients are calculated by our full-wave analysis. In Fig. 11 our results are compared with measured data, we received from Prof. Menzel, University of Ulm.

IV. Conclusion

A full-wave analysis has been performed to calculate the scattering characteristics of cascaded coplanar waveguide discontinuities. It was found that the transmission and reflection coefficients are strongly affected by metallic losses if the line geometries of the waveguide structure are in the order of the skin depth. Excellent agreement with experiments and computations of other field analysis methods is demonstrated. It is shown that waveguide discontinuities analyzed by the mode-matching approach can be modelled by an equivalent multiport, if proper testing functions are used in the enforcement of the continuity condition of the tangential field components across the discontinuity. The mode-matching equations are related to the expansions of the equivalent current densities in the discontinuity plane and to the continuity condition of the well-defined voltage and currents of quasi-TEM waves in the static approximation. This correspondence is only valid for one testing function set, thus presenting a rigorous justification of this set.

Acknowledgment

The authors would like to thank Prof. Menzel for providing the experimental data on the multilayer structure.

References

[1] T. W. Huang and T. Itoh, "The influence of metallization thickness on the characteristics of cascaded junction discontinuities of shielded coplanar type transmission line," *IEEE Trans. Microwave Theory Tech.*, vol. 41, pp. 693–697, Apr. 1993.

[2] W. Heinrich, "Full-wave analysis of conductor losses on MMIC transmission lines," *IEEE Trans. Microwave Theory Tech.*, vol. 38, pp. 1468–1472, Oct. 1990.

[3] Y. C. Shih and M. Maher, "Characterization of conductor-backed coplanar waveguides using accurate on-wafer measurement techniques," in *1990 IEEE MTT-S Int. Microwave Symp. Dig.*, pp. 1129–1132.

[4] R. Schmidt and P. Russer, "Full-wave analysis of coplanar waveguide discontinuities by partial wave synthesis," in *10th Anniversary ACES Conference*, Monterey, 1994, pp. 576–583.

[5] K. Wu, R. Vahldieck, J. L. Fikart, and H. Minkus, "The influence of finite conductor thickness and conductivity on fundamental and higher-order modes in miniature hybrid MIC's (MHMIC's) and MMIC's," *IEEE Trans. Microwave Theory Tech.*, vol. 41, pp. 421–430, Mar. 1993.

[6] F. Alessandri, G. Baini, M. Mongiardo, and R. Sorrentino, "A 3-D mode matching technique for the efficient analysis of coplanar MMIC discontinuities with finite metallization thickness," *IEEE Trans. Microwave Theory Tech.*, vol. 41, pp. 1625–1629, Sept. 1993.

[7] W. Heinrich, "Beiträge zur Simulation monolithisch integrierter Höchstfrequenzschaltungen," *Fortschrittsberichte VDI, Reihe 21: Elektrotechnik*, no. 136, 1993.

[8] R. F. Harrington, *Field Computation by Moments Methods*. Malabar: Robert E. Krieger Publishing, 1982.

[9] W. Menzel, H. Schumacher, W. Schwab, and X. Zhang, "Compact multilayer filter structures for coplanar MMIC's," *IEEE Microwave and Guide Wave Lett.*, vol. 2, pp. 497–498, Dec. 1992.

[10] Q. Xu, K. J. Webb, and R. Mittra, "Study of modal solution procedures for microstrip step discontinuities," *IEEE Trans. Microwave Theory Tech.*, vol. 37, pp. 381–386, Feb. 1989.

[11] G. V. Eleftheriades, A. S. Omar, L. P. B. Katehi, and G. M. Rebeiz, "Some important properties of waveguide junction generalized scattering matrices in the context of the mode matching technique," *IEEE Trans. Microwave Theory Tech.*, vol. 42, pp. 1896–1903, Oct. 1994.

[12] P. Penfield, Jr., R. Spence, and S. Duinker, *Tellegen's Theorem and Electrical Networks*, Research Monograph no. 58. Cambridge, MA and London, England: M.I.T. Press.

[13] R. F. Harrington, *Time Harmonic Electromagnetic Fields*. New York, NY: McGraw-Hill, 1961.

[14] J. Kessler, R. Dill, and P. Russer, "Field theory investigation of high-T_c superconducting coplanar waveguide transmission lines and resonators," *IEEE Trans. Microwave Theory Tech.*, vol. 39, pp. 1566–1574, Sept. 1991.

[15] T. S. Chu and T. Itoh, "Generalized scattering matrix method for analysis of cascaded and offset microstrip step discontinuities," *IEEE Trans. Microwave Theory Tech.*, vol. MTT-34, pp. 280–284, Feb. 1986.

[16] D. N. Zuckermann and P. Diament, "Rank reduction of ill-conditioned matrices in waveguide junction problems," *IEEE Trans. Microwave Theory Tech.*, vol. MTT-25, pp. 613–619, July 1977.
[17] J. P. Keener, *Principles of Applied Mathematics.* Reading, MA: Addison-Wesley, 1988.
[18] J. B. Murdoch, *Network Theory.* New York, NY: McGraw-Hill, 1970.

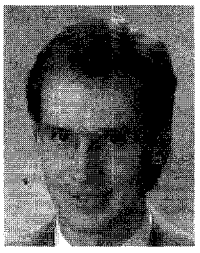

Rolf Schmidt was born in Augsburg, Germany, in 1966. He received the Dipl.Ing. degree in electrical engineering from the Technische Universität München, Germany, in 1991. Since then, he has been studying toward the Dr.Ing. degree in electrical engineering at the Lehrstuhl für Hochfrequenztechnik at the Technische Universität München.

His research interests are field theory and numerical computation of electromagnetic fields applied to MMIC structures.

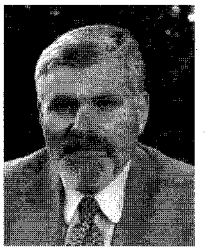

Peter Russer (SM'81-F'94) was born in Vienna, Austria, in 1943. He received the Dipl.Ing. degree in 1967 and the Dr.Tech. degree in 1971, both in electrical engineering and both from the Technische Universität in Vienna, Austria.

From 1968 to 1971, he was an Assistant Professor at the Technische Universität in Vienna. In 1971 he joined the Research Institute of AEG-Telefunken in Ulm, where he worked on fiber-optic communication, broadband solid-state electronic circuits, statistical noise analysis of microwave circuits, laser modulation, and fiber-optic gyroscopes. Since 1981 he has held the chair of Hochfrequenztechnik at the Technische Universität München. In 1990 he was Visiting Professor at the University of Ottawa. From October 1992 to March 1995 he was director of the Ferdinand-Braun-Institut für Höchstfrequenztechnik in Berlin. His current research interests are modeling and computer-aided design of integrated microwave and millimeterwave circuits, methods for electromagnetic field computation, and statistical noise analysis of microwave circuits. He is the author of more than 200 scientific papers in these areas.

Dr. Russer is a Fellow of the IEEE and member of the German Informationstechnische Gesellschaft and the Austrian and German Physical Societies. In 1979, he was corecipient of the NTG award.